（出典１）動物種による曝露期間と不確実係数（OEHHA, 2000）

動物種	平均寿命(年)	曝露期間 *			
		12%超	8%以上、12%以下	8%未満	単位
ヒヒ	55	6.6	4.4～6.6	4.4	年
ネコ	15	>94	63～94	<63	週
イヌ	15	>94	63～94	<63	週
モルモット	6	>38	25～38	<25	週
ハムスター	2.5	>16	11～16	<11	週
ヒト	70	>8.4	5.6～8.4	<5.6	年
マウス	2	>13	9～13	<9	週
ウサギ	6	>38	25～38	<25	週
ラット	2	>13	9～13	<9	週
アカゲザル	35	>4.2	2.8～4.2	<2.8	年
不確実係数設定値		1	3	10	

＊平均寿命に対する比率から算出

（註釈）

アメリカ環境保護庁(USEPA, 1994)は、平均生涯寿命の 10%未満の曝露期間で試験された亜急性曝露のデータに対しては、不確実係数(UF)として 10 を用いることを推奨している。しかしながら、その論理的根拠は明確ではなく、実際には主観的な判断に基づいて使用されてきた。そこで、カリフォルニア州環境保護庁の環境保健有害性評価局（Office of Environmental Health Hazard Assessment: OEHHA, 2000）は、一貫性のある曝露補正の不確実係数を提案している。この提案によるアプローチは、平均寿命に対する比率に基づき、(1)平均寿命の 8%未満では不確実係数 10、(2)同 8～12%以下では不確実係数 3、同 12%超では不確実係数 1 としている。本論では、この提案によるアプローチが最も実用的であると判断し、この方法を採用した。

（参考文献）

Azuma K, Uchiyama I, Ikeda K. 2007. The risk screening for indoor air pollution chemicals in Japan. Risk Anal, 27(6), 1623–1638.

Azuma K, Uchiyama I, Uchiyama S, et al., 2016. Assessment of inhalation exposure to indoor air pollutants: Screening for health risks of multiple pollutants in Japanese dwellings. Environ Res, 145, 39–49.

Office of Environmental Health Hazard Assessment (2000) Air Toxics Hot Spots Program, Risk Assessment Guidelines Part III, Technical Support Document for the Determination of Noncancer Chronic Reference Exposure Levels, 41pages

１２．初期リスク評価結果

導出した RfC をもとに、国立衛研で実施してきた個々の物質の室内濃度に対して MOE (Margin of Exposure)を算出した（表１２－１）。曝露濃度は、初期リスク評価であることから、各実態調査の最大濃度を用いた。MOE が 1 未満（優先度 A）であれば、詳細な調査が必要であると判断される。MOE が 1 以上 10 未満（優先度 B）であれば、さらなる情報収集が必要と判断される。MOE が 10 以上（優先度 C）であれば、情報収集の必要がないと判断される（Azuma et al., 2016）。今後の詳細調査の優先度を表１２－２にまとめた。

表１２－１　初期リスク評価結果の一覧

		調査世帯	建築	最大室内濃度 (μg Toluene/m3)	RfC (μg/m3)	MOE	濃度データの出典
2-エチルヘキサノール	2013 全国夏	93	既築	130	80	0.6	NIHS (2014)
	2013 東京都	100	既築	69	80	1.2	NIHS (2014)
	2012 全国夏	111	既築	122	80	0.7	NIHS (2013b)
	2012 全国冬	111	既築	20	80	4.0	NIHS (2013b)
	2011 全国冬	101	既築	36	80	2.2	NIHS (2013a)
TXIB	2013 全国夏	93	既築	64	100	1.6	NIHS (2014)
	2013 東京都	100	既築	10	100	10.0	NIHS (2014)
	2012 全国夏	111	既築	12	100	8.3	NIHS (2013b)
	2012 全国冬	111	既築	11	100	9.1	NIHS (2013b)
	2012 全国新築冬	45	新築	661	100	0.2	NIHS (2013b)
テキサノール	2013 全国夏	93	既築	59	3300	55.9	NIHS (2014)
	2012 全国夏	111	既築	35	3300	94.3	NIHS (2013b)
	2012 全国冬	111	既築	22	3300	150.0	NIHS (2013b)
	2012 全国新築冬	45	新築	837	3300	3.9	NIHS (2013b)
D4	2012 全国新築冬	45	新築	78	250	3.2	NIHS (2013b)
D5	2013 全国夏	93	既築	690	268	0.4	NIHS (2014)
	2013 東京都	100	既築	280	268	1.0	NIHS (2014)
	2012 全国夏	111	既築	488	268	0.5	NIHS (2013b)
	2012 全国冬	111	既築	147	268	1.8	NIHS (2013b)
	2012 全国新築冬	45	新築	48	268	5.6	NIHS (2013b)
プロピレングリコール	2013 全国夏	93	既築	51	95	1.9	NIHS (2014)
	2013 東京都	100	既築	32	95	3.0	NIHS (2014)
	2012 全国夏	111	既築	93	95	1.0	NIHS (2013b)
	2012 全国冬	111	既築	17	95	5.6	NIHS (2013b)
1,3-ブタンジオール	2013 全国夏	93	既築	110	25000	227.3	NIHS (2014)
	2013 東京都	100	既築	130	25000	192.3	NIHS (2014)
	2012 全国夏	111	既築	93	25000	268.8	NIHS (2013b)
	2012 全国冬	111	既築	25	25000	1000.0	NIHS (2013b)
酢酸エチル	2013 全国夏	93	既築	170	76	0.4	NIHS (2014)
	2013 東京都	100	既築	64	76	1.2	NIHS (2014)
	2012 全国新築冬	45	新築	151	76	0.5	NIHS (2013b)
酢酸ブチル	2012 全国夏	111	既築	63	1429	22.7	NIHS (2013b)
	2012 全国冬	111	既築	33	1429	43.3	NIHS (2013b)
	2012 全国新築冬	45	新築	664	1429	2.2	NIHS (2013b)

（室内最大濃度データの出典）

NIHS. 2013a. Report at the 12th meeting, Committee on sickhouse syndrome: indoor air pollution, Ministry of Health, Labour and Welfare. National Institute of Health Sciences, Tokyo, Feb. 18, 2013.

NIHS. 2013b. Report at the 17th meeting, Committee on sickhouse syndrome: indoor air pollution, Ministry of Health, Labour and Welfare. National Institute of Health Sciences, Tokyo, Aug. 1, 2013.

NIHS. 2014. Report at the 18th meeting, Committee on sickhouse syndrome: indoor air pollution, Ministry of Health, Labour and Welfare. National Institute of Health Sciences, Tokyo, Mar. 17, 2014.

表１２－２　今後の詳細リスク評価の優先度のまとめ

	優先度	室内環境汚染物質
既築住宅	A（詳細評価）	2-エチルヘキサノール（夏期） D5（夏期） 酢酸エチル（夏期）
	B（情報収集）	2-エチルヘキサノール（冬期、秋期） TXIB（夏期、冬期、秋期） D5（冬期、秋期） プロピレングリコール（夏期、冬期、秋期） 酢酸エチル（秋期）
	C（静観）	テキサノール（夏期、冬期） 1,3-ブタンジオール（夏期、冬期、秋期） 酢酸ブチル（夏期、冬期）
新築住宅	A（詳細評価）	TXIB（冬期） 酢酸エチル（冬期）
	B（情報収集）	テキサノール（冬期） D4（冬期） D5（冬期） 酢酸ブチル（冬期）
	C（静観）	

III. 研究成果の刊行に関する一覧表

研究成果の刊行に関する一覧表

発表者氏名	論文タイトル名	発表誌名	巻号	ページ	出版年
Mukai M. Isobe T. Okada K. Murata M. Shigeyama M. Hanioka N.	Species and sex differences in propofol glucuronidation in liver microsomes of humans, monkeys, rats and mice.	*Pharmazie*	70	466–470	2015
Miyake Y. Hirose R. Isobe T. Hanioka N.	Molecular cloning and functional analysis of minipig UDP-glucuronosyltransferase 1A6.	*Xenobiotica*	46(3)	193–199	2016
Kishi N. Takasuka A. Kokawa Y. Isobe T. Taguchi M. Shigeyama M. Murata M. Suno M. Hanioka N.	Raloxifene glucuronidation in liver and intestinal microsomes of humans and monkeys: contribution of UGT1A1, UGT1A8, and UGT1A9.	*Xenobiotica*	46(4)	289–295	2016
Hanioka N. Kinashi Y. Tanaka-Kagawa T. Isobe T. Jinno H.	Glucuronidation of mono(2-ethylhexyl) phthalate in humans: roles of hepatic and intestinal UDP-glucuronosyltransferases.	*Arch Toxicol*		doi: 10.1007/s00204-016-1708-9.	*in press*

Hanioka N. Isobe T. Kinashi Y. Tanaka-Kagawa T. Jinno H.	Hepatic and intestinal glucuronidation of mono(2-ethylhexyl) phthalate, an active metabolite of di(2-ethylhexyl) phthalate, in humans, dogs, rats and mice: an in vitro analysis using microsomal fractions.	*Arch Toxicol*		doi: 10.1007/s00204-015-1619-1.	*in press*
Phuong NL. Ito K.	Investigation of Flow Pattern in a Realistic Replica Model of Human Respiratory Tract using PIV.	*Building and Environment*	94	504-515	2015
Phuong NL. Yamashita M. Yoo SJ. Ito K.	Prediction of convective heat transfer coefficient of human upper and lower airway surfaces in steady and unsteady breathing conditions.	*Building and Environment*	100	172-185	2016
Kawakami T. Isama K. Ikarashi Y.	Survey of isothiazolinones and other preservatives in household wet tissue products in Japan.	*J. Environ. Chem*	25	207-214	2015

Hirata-Koizumi M. Fujii S. Hina K. Matsumoto M. Takahashi M. Ono A. Hirose A.	Repeated dose and reproductive/developmental toxicity of long-chain perfluoroalkyl carboxylic acids in rats: perfluorohexadecanoic acid and perfluorotetradecanoic acid.	*Fundam Toxicol Sci*	2(4)	177-190	2015
Ono A. Kobayashi K. Serizawa H. Kawamura T. Kato H. Matsumoto M. Takahashi M. Hirata-Koizumi M. Matsushima Y. Hirose A.	A repeated dose 28-day oral toxicity study of β-bromostyrene in rats.	*Fundam. Toxicol Sci*	2(4)	191-200	2015
Kato H. Fujii S. Takahashi M. Matsumoto M. Hirata-Koizumi M. Ono A. Hirose A.	Repeated dose and reproductive/developmental toxicity of perfluorododecanoic acid in rats.	*Environ Toxicol*	30	1244-1263	2015
Azuma K, Tanaka-Kagawa T, Jinno H.	Health risk assessment of inhalation exposure to 2-ethylhexanol, 2,2,4-trimethyl-1,3-pentanediol diisobutyrate, and texanol in indoor environments.	*Proceedings of the 14th international conference of Indoor Air Quality and Climate*			*in press*

IV. 研究成果の刊行物・別刷

Faculty of Pharmaceutical Sciences[1], Okayama University, Okayama; Department of Biochemical Toxicology[2], Department of Clinical Pharmacy[3], Yokohama University of Pharmacy, Yokohama, Japan

Species and sex differences in propofol glucuronidation in liver microsomes of humans, monkeys, rats and mice

M. Mukai[1], T. Isobe[2], K. Okada[3], M. Murata[3], M. Shigeyama[3], N. Hanioka[2]

Received January 23, 2015, accepted February 27, 2015

Dr. Nobumitsu Hanioka, Professor, Department of Biochemical Toxicology, Yokohama University of Pharmacy, 601 Matano-cho, Totsuka-ku, Yokohama 245-0066, Japan
nhanioka@hamayaku.ac.jp

Pharmazie 70: 466–470 (2015) *doi: 10.1691/ph.2015.5525*

Propofol (2,6-diisopropylphenol) is a short-acting anesthetic commonly used in clinical practice, and is rapidly metabolized into glucuronide by UDP-glucuronosyltransferase (UGT). In the present study, propofol glucuronidation was examined in the liver microsomes of male and female humans, monkeys, rats, and mice. The kinetics of propofol glucuronidation by liver microsomes fit the substrate inhibition model for humans and mice, the Hill model for monkeys, and the isoenzyme (biphasic) model for rats. The K_m, V_{max}, and CL_{int} values of human liver microsomes were 50 μM, 5.6 nmol/min/mg protein, and 110 μL/min/mg protein, respectively, for males, and 46 μM, 6.0 nmol/min/mg protein, and 130 μL/min/mg protein, respectively, for females. The rank order of the CL_{int} or CL_{max} (*in vitro* clearance) values of liver microsomes was mice » humans > monkeys > rats (high-affinity phase) » rats (low-affinity phase) in both males and females. Although no significant sex differences were observed in the values of kinetic parameters in any animal species, the *in vitro* clearance values of liver microsomes were males < females in humans, males = females in rats (low-affinity phase), and males > females in monkeys, rats (high-affinity phase), and mice. These results demonstrated that the kinetic profile of propofol glucuronidation by liver microsomes markedly differed among humans, monkeys, rats, and mice, and suggest that species and sex differences exist in the roles of UGT isoform(s), including UGT1A9, involved in its metabolism.

1. Introduction

Propofol (2,6-diisopropylphenol) is widely used as an intravenous anesthetic agent. It is rapidly eliminated from the body, and conjugation catalyzed by UDP-glucuronosyltransferase (UGT) in the liver is the main pathway for its metabolism in humans (Langley and Heel 1988; Vanlersberghe and Camu 2008). UGT1A9 has been identified as the predominant isoform for the glucuronidation of propofol in humans (Soars et al. 2003; Court 2005; Kiang et al. 2005). Human UGT1A9 is expressed not only in the liver, but also in extrahepatic tissues such as the kidney and small intestine (Ohno and Nakajin 2009; Harbourt et al. 2012). We recently reported that UGT1A9 expressed in the kidney as well as in the liver played an important role in propofol glucuronidation (Mukai et al. 2014). UGT1A8 expressed mainly in the digestive organs, but not in the liver has also been shown to glucuronidate propofol (Cheng et al. 1999; Kiang et al. 2005). *In vivo* studies previously identified marked species differences in the pharmacokinetic and metabolic profiles of propofol among rats, rabbits, and dogs (Simons et al. 1991, 1992; Cockshott et al. 1992), and these differences have been attributed to the levels of expression and function of the UGT isoform(s) responsible for propofol glucuronidation in each animal species. Several cDNAs of rodents and/or monkeys that encode the orthologs of human UGT1A8 and UGT1A9 have been cloned (http://www.flinders.edu.au/medicine/sites/clinical-pharmacology/ugt-homepage.cfm), and the functions of each UGT enzyme coded by cDNA have been characterized (Ritter 2000; Kiang at al. 2005). Previous studies suggested that large interindividual variability existed in the expression levels of UGT1A9 mRNA and protein in the livers of humans (Izukawa et al. 2009; Oda et al. 2012), and these variations may affect the plasma concentration, efficacy, and side-effects of propofol. Loryan et al. (2012) and Choong et al. (2013) demonstrated that the AUC of propofol glucuronide after a single bolus dose was 1.3-fold higher in female patients than in male patients. Thus, several *in vivo* studies have reported notable species and sex differences in propofol glucuronidation. However, the *in vitro* glucuronidation of propofol has not yet been examined in mammals. The aim of the present study was to clarify species and sex differences in the glucuronidation of propofol in the liver microsomes of humans, monkeys, rats, and mice.

2. Investigations and results

2.1. Propofol glucuronidation activities in liver microsomes

The glucuronidation activities of propofol in human, monkey, rat, and mouse liver microsomes were determined at a substrate concentration of 50 μM (Fig. 1). Glucuronidation activities in male and female human liver microsomes were 2.7 and 3.0 nmol/min/mg protein, respectively. Activities in monkey liver microsomes were 1.6-fold for males and 1.3-fold for females

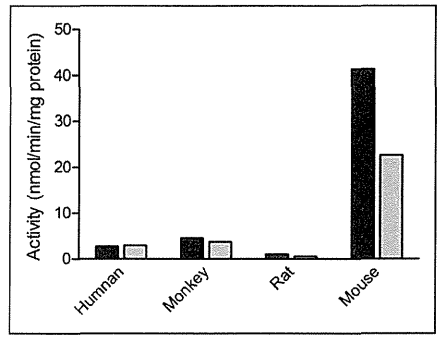

Fig. 1: Propofol glucuronidation activities in human, monkey, rat amd mouse liver microsomes. The substrate concentrations used was 50 μM. Each column represents the mean of three separate experiments performed in duplicate. ■, males; ▒, females.

of those in human liver microsomes, respectively. Activities in male and female rat liver microsomes were 37% and 18% of those in human liver microsomes, respectively. Activities were markedly higher in male and female mouse liver microsomes (15- and 7.7-fold, respectively) than in human liver microsomes. Glucuronidation activities in male and female liver microsomes were similar between humans and monkeys. In rats and mice, activities were approximately 2-fold higher in male liver microsomes than in female liver microsomes.

2.2. Kinetics for propofol glucuronidation by liver microsomes

A kinetic analysis of propofol glucuronidation by the liver microsomes of humans, monkeys, rats, and mice was performed to obtain more detailed information. The plots (V-[S] and V-V/[S] plots) and parameters of the kinetics tested are shown in Figs. 2–5 and the Table 1, respectively. The kinetics for propofol glucuronidation by male and female human liver microsomes exhibited substrate inhibition with *K*si values of 530–550 μM. The K_m, V_{max}, and CL_{int} values of male human liver microsomes were 50 μM, 5.6 nmol/min/mg protein, and 110 μL/min/mg protein, respectively. The parameter values of female human liver microsomes were similar to those of male human liver microsomes. The kinetics by male and female monkey liver microsomes fit the Hill model with n of 1.5–1.6, and the S_{50}, V_{max}, and CL_{max} values of male monkey liver microsomes were 71 μM, 13 nmol/min/mg protein, and 93 μL/min/mg protein, respectively. The parameter values of female monkey liver microsomes were similar to those of male monkey liver microsomes.

Propofol glucuronidation by male and female rat liver microsomes exhibited isoenzyme (biphasic) kinetics. The K_m, V_{max}, and CL_{int} values of male rat liver microsomes were 8.0 μM, 0.6 nmol/min/mg protein, and 72 μL/min/mg protein for the high-affinity phase, and 170 μM, 2.1 nmol/min/mg protein, and 13 μL/min/mg protein for the low-affinity phase, respectively. The K_m and V_{max} values of female rat liver microsomes were lower than those of male rat liver microsomes (56% and 26% for the high-affinity phase, and 75% and 64% for high-affinity phase, respectively). The results revealed that the CL_{int} value of female rat liver microsomes in the high-affinity phase was approximately 50% that of male rat liver microsomes, whereas the value in the low-affinity phase was similar to that of male

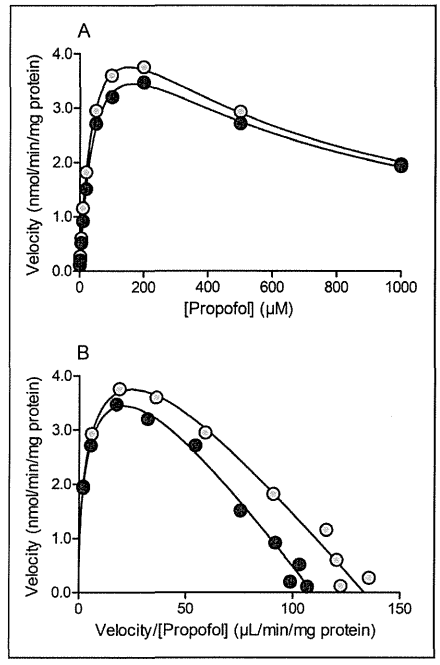

Fig. 2: Kinetics of propofol glucuronidation by human liver microsomes. Substrate concentrations were 1–1000 μM. Each point represents the mean of three separate experiments. •, males; ○, females. (A) V-[S] plots; (B) V-V/[S] plots.

rat liver microsomes. The kinetics by male and female mouse liver microsomes exhibited substrate inhibition with *K*si values of 75–110 μM. The K_m, V_{max}, and CL_{int} values of male mouse liver microsomes were 40 μM, 97 nmol/min/mg protein, and 2400 μL/min/mg protein, respectively; and these values in female mouse liver microsomes were 76%, 58%, and 76% of those in male mouse liver microsomes, respectively.

3. Discussion

Propofol is intravenously administered for anesthetic induction and maintenance. It is rapidly metabolized, with the majority of the dose being excreted into urine as propofol glucuronide in humans (Langleyand and Heel 1988; Vanlersberghe and Camu 2008). Although *in vivo* studies have been performed on species and sex differences in propofol glucuronidation in mammals (Simons et al. 1991, 1992; Cockshott et al. 1992; Loryan et al. 2012; Choong et al. 2013), there is no information on the *in vitro* glucuronidation of propofol. Therefore, we herein examined the glucuronidation of propofol in the liver microsomes of humans, monkeys, rats, and mice.

To obtain basic information on species and sex differences in propofol glucuronidation, propofol glucuronidation activities were initially determined in the liver microsomes of humans, monkeys, rats, and mice at a single substrate concentration of 50 μM. The rank order of these activities in liver microsomes was mice » monkeys > humans > rats in both males and females. UGT1A9 has been identified as the predominant isoform for the

Table 1: Kinetic parameters for propofol glucuronidation by human, monkey, rat and mouse liver microsomes

	K_m or S_{50} (μM)	V_{max} (nmol/min/mg protein)	n	CL_{int} or CL_{max} (μL/min/mg protein)	K_{si} (μM)	Model
Human						
Male	50.2 ± 9.6	5.62 ± 0.64		110 ± 13	546 ± 105	Substrate inhibition
Female	45.8 ± 8.8	6.02 ± 0.59		134 ± 15	531 ± 115	Substrate inhibition
Monkey						
Male	71.4 ± 8.2	12.5 ± 1.0	1.61 ± 0.23	92.5 ± 8.7		Hill
Female	83.1 ± 9.5	11.7 ± 0.5	1.53 ± 0.16	75.1 ± 3.6		Hill
Rat						
Male						Isoenzyme
High-affinity phase	8.00 ± 1.22	0.58 ± 0.12		72.0 ± 8.9		
Low-affinity phase	169 ± 20	2.07 ± 0.37		12.5 ± 3.2		
Female						Isoenzyme
High-affinity phase	4.45 ± 1.65	0.15 ± 0.05		35.4 ± 8.9		
Low-affinity phase	127 ± 36	1.33 ± 0.20		12.9 ± 7.0		
Mouse						
Male	40.1 ± 1.9	97.1 ± 7.8		2420 ± 180	114 ± 19	Substrate inhibition
Female	30.5 ± 4.3	56.2 ± 6.2		1850 ± 130	75.4 ± 7.5	Substrate inhibition

Each value represents the mean ± SD of three separate experiments.

glucuronidation of propofol in humans (Court 2005; Kiang et al. 2005), and is extensively expressed in hepatic and extrahepatic tissues (Ohno and Nakajin 2009; Harbourt et al. 2012; Fallon et al. 2013). The cDNAs of monkeys and mice that encode the ortholog of human UGT1A9 have been cloned; however, rat UGT1A9 cDNA has been identified as a pseudogene (Emi et al. 1995; Albert et al. 1999; Zhang et al. 2004). The weak

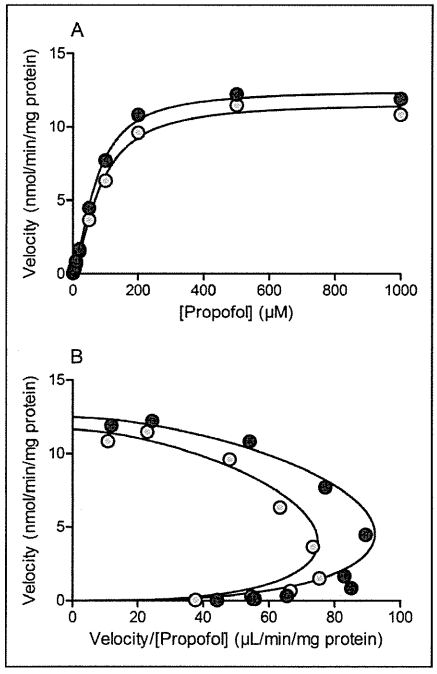

Fig. 3: Kinetics of propofol glucuronidation by monkey liver microsomes. Substrate concentrations were 1–1000 μM. Each point represents the mean of three separate experiments. •, males; ○, females. (A) V-[S] plots; (B) V-V/[S] plots.

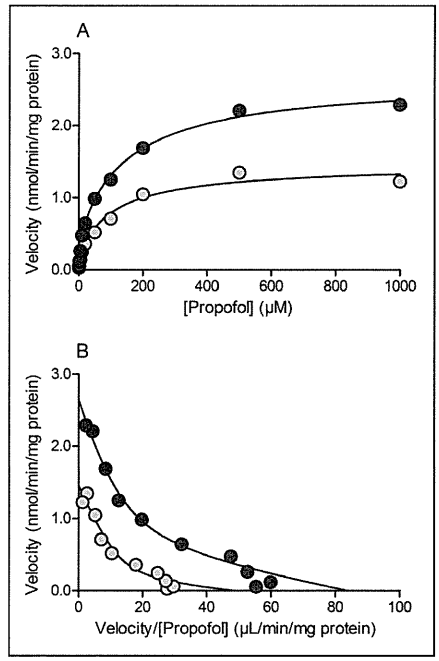

Fig. 4: Kinetics of propofol glucuronidation by rat liver microsomes. Substrate concentrations were 1–1000 μM. Each point represents the mean of three separate experiments. •, males; •, females. (A) V-[S] plots; (B) V-V/[S] plots.

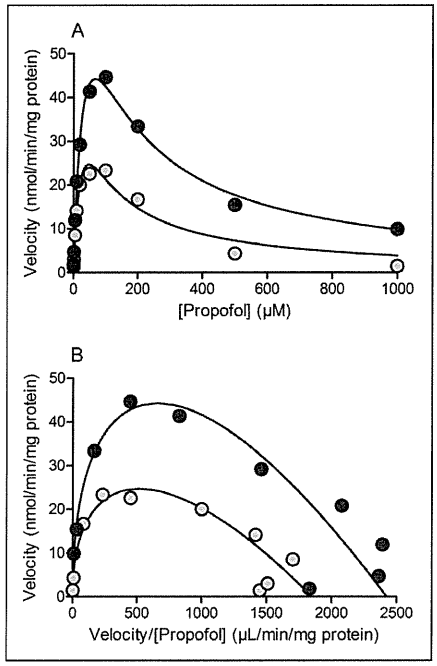

Fig. 5: Kinetics of propofol glucuronidation by mouse liver microsomes. Substrate concentrations were 1–1000 μM. Each point represents the mean of three separate experiments. •, males; ○, females. (A) V-[S] plots; (B) V-V/[S] plots.

glucuronidation of propofol by rat liver microsomes has been attributed to a deficiency in the UGT1A9 enzyme in rats.

Kinetic analyses of propofol glucuronidation by the liver microsomes of humans, monkeys, rats, and mice were subsequently performed at a broad range of substrate concentrations. Soars et al. (2003) previously reported that the kinetics of propofol glucuronidation by human liver microsomes fit the Michaelis–Menten model with K_m values of 190–280 μM. In the present study, the kinetics by both male and female human liver microsomes exhibited substrate inhibition. Although no marked differences were observed in the values of kinetic parameters between male and female human liver microsomes, the CL_{int} value of female human liver microsomes was 1.2-fold higher than that of male human liver microsomes, supporting the *in vivo* studies by Loryan et al. (2012) and Choong et al. (2013). The kinetics for propofol glucuronidation by monkey liver microsomes exhibited a distinctive "hook" on V-V/[S] plots, suggesting the mechanism of allosteric activation, and the data obtained were found to fit the Hill model best. The kinetic profile differed from that of human liver microsomes, although the *in vitro* clearance values were similar for both sexes. We recently reported that the *in vitro* clearance value for propofol glucuronidation by recombinant monkey UGT1A9 was 2% of recombinant human UGT1A9 (Yamamoto et al. 2014). Our previous and present results indicated that UGT isoform(s), except for UGT1A9, predominantly contributed to the glucuronidation of propofol in the monkey liver. On the other hand, the S_{50}, V_{max}, CL_{max}, and n values of male and female monkey liver microsomes were similar, and no marked sex difference was observed in the *in vitro* kinetics of propofol glucuronidation.

In rat liver microsomes, the kinetics for propofol glucuronidation fit a biphasic model, suggesting the contribution of one or more UGT isoforms for its metabolism. The V_{max} and CL_{int} values for the low- and high-affinity phases were the lowest among the liver microsomes of the animal species examined in this study in both males and females. Since the UGT1A9 enzyme is deficient in rats (Emi et al. 1995), plural UGT isoforms, except for UGT1A9, glucuronidated propofol. The kinetic profile of substrate inhibition was observed in mouse as well as in human liver microsomes, and the K_{si} values obtained were approximately 10–20% of human liver microsomes. The K_m values of mouse liver microsomes were similar to those of human liver microsomes, whereas the V_{max} and CL_{int} values were approximately 15–20-fold higher than those of human liver microsomes. The V_{max} and CL_{int} values of female mouse liver microsomes were approximately 25–40% lower than those of male mouse liver microsomes. These results imply that UGT1A9 expression levels were markedly higher in the mouse liver than in the human liver, and differed between males and females.

The mRNA and protein of human UGT1A9 were previously found to be expressed in not only the liver, but also in extrahepatic tissues such as the kidney and intestines (Ohno and Nakajin 2009; Harbourt et al. 2012; Fallon et al. 2013). We recently reported the *in vitro* glucuronidation of propofol by human liver, intestinal, and kidney microsomes, and found that UGT1A9 expressed in the kidney as well as in the liver played an important role in propofol glucuronidation (Mukai et al. 2014). Additionally, the efficiency of propofol glucuronidation by intestinal microsomes was suggested to less than that of liver and kidney microsomes. Human UGT1A8, which is mainly expressed in the intestines, has also been shown to contribute to the glucuronidation of propofol, although the *in vitro* clearance value is estimated to be lower than that of UGT1A8 (Cheng et al. 1999; Soars et al. 2003; Court 2005; Kiang et al. 2005). Therefore, UGT1A9 was confirmed to be the main enzyme responsible for the glucuronidation of propofol in the human liver. Information on the tissue distribution of the mRNAs and proteins of each UGT isoform is limited in monkeys, rats, and mice. Among the cDNAs of monkeys, rats, and encoding orthologs of human UGT1A8 and UGT1A9 cloned to date (http://www.flinders.edu.au/medicine/sites/clinical-pharmacology/ugt-homepage.cfm), rat UGT1A9 has been identified as a pseudogene (Emi et al. 1995). Further studies are required to clarify the roles of hepatic and extrahepatic UGT isoforms including UGT1A8 and UGT1A9 in propofol glucuronidation using recombinant enzymes of each animal species.

In conclusion, propofol glucuronidation in male and female human, monkey, rat, and mouse liver microsomes was examined using a kinetic analysis. The kinetics for propofol glucuronidation by liver microsomes fit the substrate inhibition model for humans and mice, the Hill model for monkeys, and the biphasic model for rats. Species differences in the *in vitro* clearance values of liver microsomes were mice » humans > monkeys > rats (the high-affinity phase) » rats (the low-affinity phase) in both sexes. Sex differences in the *in vitro* clearance values of liver microsomes were males < females in humans, males = females in rats (the low-affinity phase), and males > females in monkeys, rats (the high-affinity phase), and mice. These results demonstrated that the kinetic profile of propofol glucuronidation by liver microsomes markedly differed between humans, monkeys, rats, and mice, and suggested that species and sex differences exist in the roles of UGT isoform(s), including UGT1A9, involved in its metabolism.

4. Experimental

4.1. Materials

Propofol and propofol glucuronide were obtained from Santa Cruz Biotechnology (Santa Cruz, CA, USA). The pooled liver microsomes of humans (race, Caucasian, Hispanic, and African American; age, 20–78 years old), monkeys (strain, cynomolgus; age, 3–8 years old), rats (strain, Wistar; age, 8–10 weeks old), and mice (strain, CD1; age, 8–11 weeks old) were purchased from XenoTech (Lenexa, KS, USA). All other chemicals and reagents used were of the highest quality commercially available.

4.2. Assay for propofol glucuronidation activity

Propofol glucuronidation activities were determined in the liver microsomes of humans, monkeys, rats, and mice according to a previously described method with minor modifications (Mukai et al. 2014). The incubation mixture contained propofol (1–1000 μM), microsomes (200 μg protein/mL for human liver microsomes, 100 μg protein/mL for monkey liver microsomes, 500 μg protein/mL for rat liver microsomes, and 10 μg protein/mL for mouse liver microsomes), alamethicin (20 μg/mL), 10 mM $MgCl_2$, and 2 mM UDP-glucuronic acid in a final volume of 200 μL of 50 mM Tris-HCl buffer (pH 7.4). After preincubation for 2 min at 37 °C, the reaction was initiated by adding UDP-glucuronic acid. Incubation was performed for 20 min at 37 °C and terminated by adding 50 μL of 10% phosphoric acid and vortexing. Propofol was dissolved in methanol/dimethyl sulfoxide (50:50, v/v) and the final concentration of the organic solvent (methanol and dimethyl sulfoxide) in the incubation mixture was 1% (v/v). The samples were centrifuged at 12000 g for 10 min at 4 °C. The supernatant was filtered with a polytetrafluoroethylene membrane filter (0.45 μm), and 50 μL of the filtrate was subjected to high-performance liquid chromatography with an Inertsil ODS-SP column (4.6 mm i.d. × 150 mm; GL Sciences, Tokyo, Japan). The column was maintained at 40 °C. Propofol glucuronide was isocratically eluted with 0.1% acetic acid/acetonitrile (60:40, v/v) at a flow rate of 1.0 mL/min. UV detection was performed at 220 nm. Standard curve samples spiked with propofol glucuronide were prepared in the same manner as incubation samples.

4.3. Data analysis

Kinetic parameters (K_m or S_{50}, and V_{max}), the Hill coefficient (n), and K_{si} for propofol glucuronidation were calculated by constructing velocity versus substrate concentration (V-[S]) plots using SigmaPlot v8.02 software (Systat Software, San Jose, CA, USA). The kinetic profile was estimated from the respective coefficient of determination and/or Akaike's information criterion values for the Michaelis–Menten, isoenzyme, substrate inhibition, and Hill equations. *In vitro* clearance values were CL_{int} (V_{max}/K_m) or CL_{max} ($V_{max}/S_{50}*(n\text{-}1)/(n(n\text{-}1)^{1/n})$). All values are expressed as the mean ± SD of three separate experiments performed in duplicate.

Acknowledgements: This work was supported in part by a Grant-in-Aid for Scientific Research (26281028) from the Japan Society for the Promotion of Science.

References

Albert C, Vallée M, Beaudry G, Bélanger A, Hum DW (1999) The monkey and human uridine diphosphate-glucuronosyltransferase UGT1A9, expressed in steroid target tissues, are estrogen-conjugating enzymes. Endocrinology 140: 3292–3302.

Cheng Z, Radominska-Pandya A, Tephly TR (1999) Studies on the substrate specificity of human intestinal UDP-glucuronosyltransferases 1A8 and 1A10. Drug Metab Dispos 27: 1165–1170.

Choong E, Loryan I, Lindqvist M, Nordling Å, el Bouazzaoui S, van Schaik RH, Johansson I, Jakobsson J, Ingelman-Sundberg M (2013) Sex difference in formation of propofol metabolites: a replication study. Basic Clin Pharmacol Toxicol 113: 126–131.

Cockshott ID, Douglas EJ, Plummer GF, Simons PJ (1992) The pharmacokinetics of propofol in laboratory animals. Xenobiotica 22: 369–375.

Court MH (2005) Isoform-selective probe substrates for *in vitro* studies of human UDP-glucuronosyltransferases. Methods Enzymol 400: 104–116.

Emi Y, Ikushiro S, Iyanagi T (1995) Drug-responsive and tissue-specific alternative expression of multiple first exons in rat UDP-glucuronosyltransferase family 1 (UGT1) gene complex. J Biochem 117: 392–399.

Fallon JK, Neubert H, Goosen TC, Smith PC (2013) Targeted precise quantification of 12 human recombinant uridine-diphosphate glucuronosyl transferase 1A and 2B isoforms using nano-ultra-high-performance liquid chromatography/tandem mass spectrometry with selected reaction monitoring. Drug Metab Dispos 41: 2076–2080.

Harbourt DE, Fallon JK, Ito S, Baba T, Ritter JK, Glish GL, Smith PC (2012) Quantification of human uridine-diphosphate glucuronosyl transferase 1A isoforms in liver, intestine, and kidney using nanobore liquid chromatography-tandem mass spectrometry. Anal Chem 84: 98–105.

Izukawa T, Nakajima M, Fujiwara R, Yamanaka H, Fukami T, Takamiya M, Aoki Y, Ikushiro S, Sakaki T, Yokoi T (2009) Quantitative analysis of UDP-glucuronosyltransferase (UGT) 1A and UGT2B expression levels in human livers. Drug Metab Dispos 37: 1759–1768.

Kiang TK, Ensom MH, Chang TK (2005) UDP-glucuronosyltransferases and clinical drug-drug interactions. Pharmacol Ther 106: 97–132.

Langley MS, Heel RC (1988) Propofol. A review of its pharmacodynamic and pharmacokinetic properties and use as an intravenous anaesthetic. Drugs 35: 334–372.

Loryan I, Lindqvist M, Johansson I, Hiratsuka M, van der Heiden I, van Schaik RH, Jakobsson J, Ingelman-Sundberg M (2012) Influence of sex on propofol metabolism, a pilot study: implications for propofol anesthesia. Eur J Clin Pharmacol 68: 397–406.

Mukai M, Tanaka S, Yamamoto K, Murata M, Okada K, Isobe T, Shigeyama M, Hichiya H, Hanioka N (2014) *In vitro* glucuronidation of propofol in microsomal fractions from human liver, intestine and kidney: tissue distribution and physiological role of UGT1A9. Pharmazie 69: 829–832.

Oda S, Nakajima M, Hatakeyama M, Fukami T, Yokoi T (2012) Preparation of a specific monoclonal antibody against human UDP-glucuronosyltransferase (UGT) 1A9 and evaluation of UGT1A9 protein levels in human tissues. Drug Metab Dispos 40: 1620–1627.

Ohno S, Nakajin S (2009) Determination of mRNA expression of human UDP-glucuronosyltransferases and application for localization in various human tissues by real-time reverse transcriptase-polymerase chain reaction. Drug Metab Dispos 37: 32–40.

Ritter JK (2000) Roles of glucuronidation and UDP-glucuronosyltransferases in xenobiotic bioactivation reactions. Chem Biol Interact 129: 171–193.

Simons PJ, Cockshott ID, Douglas EJ, Gordon EA, Knott S, Ruane RJ (1991) Species differences in blood profiles, metabolism and excretion of ^{14}C-propofol after intravenous dosing to rat, dog and rabbit. Xenobiotica 21: 1243–1256.

Simons PJ, Cockshott ID, Glen JB, Gordon EA, Knott S, Ruane RJ (1992) Disposition and pharmacology of propofol glucuronide administered intravenously to animals. Xenobiotica 22: 1267–1273.

Soars MG, Ring BJ, Wrighton SA (2003) The effect of incubation conditions on the enzyme kinetics of udp-glucuronosyltransferases. Drug Metab Dispos 31:762–767.

Vanlersberghe C, Camu F. Propofol (2008) Handb Exp Pharmacol 182: 227–252.

Yamamoto K, Mukai M, Nagaoka K, Hayashi K, Hichiya H, Okada K, Murata M, Shigeyama M, Narimatsu S, Hanioka N (2014) Functional characterization of cynomolgus monkey UDP-glucuronosyltransferase 1A9. Eur J Drug Metab Pharmacokinet 39: 195–202.

Zhang T, Haws P, Wu Q (2004) Multiple variable first exons: a mechanism for cell- and tissue-specific gene regulation. Genome Res 14: 79–89.

http://tandfonline.com/ixen
ISSN: 0049-8254 (print), 1366-5928 (electronic)

Xenobiotica

Xenobiotica, 2016; 46(3): 193–199
 DOI: 10.3109/00498254.2015.1060373

informa
healthcare

RESEARCH ARTICLE

Molecular cloning and functional analysis of minipig UDP-glucuronosyltransferase 1A6

Yuuka Miyake[1], Riho Hirose[1], Takashi Isobe[2], and Nobumitsu Hanioka[2]

[1]*Faculty of Pharmaceutical Sciences, Okayama University, Okayama, Japan and* [2]*Department of Biochemical Toxicology, Yokohama University of Pharmacy, Yokohama, Japan*

Abstract

1. UDP-glucuronosyltransferase 1A6 (UGT1A6) plays important roles in the glucuronidation of numerous drugs, environmental pollutants, and endogenous substances. Minipigs have been used as experimental animals in pharmacological and toxicological studies because many of their physiological characteristics are similar to those of humans. The aim of the present study was to examine similarities and differences in the enzymatic properties of UGT1A6 between humans and minipigs.
2. Minipig UGT1A6 (mpUGT1A6) cDNA was cloned by the RACE method, and the corresponding proteins were expressed in insect cells. The enzymatic function of mpUGT1A6 was analyzed by the kinetics of serotonin glucuronidation.
3. Amino acid homology between human UGT1A6 (hUGT1A6) and mpUGT1A6 was 79.9%. The kinetics of serotonin glucuronidation by recombinant hUGT1A6 and mpUGT1A6 enzymes fit the Michaelis–Menten equation. The K_m, V_{max}, and CL_{int} values of hUGT1A6 were 10.5 mM, 4.04 nmol/min/mg protein, and 0.39 μL/min/mg protein, respectively. The K_m value of mpUGT1A6 was similar to that of hUGT1A6, whereas the V_{max} and CL_{int} values of mpUGT1A6 were approximately 2-fold higher than those of hUGT1A6.
4. These results suggest that the enzymatic properties of UGT1A6 enzymes are moderately different between humans and minipigs.

Keywords

Glucuronidation, minipig, serotonin, UDP-glucuronosyltransferase, UGT1A6

History

Received 15 May 2015
Revised 3 June 2015
Accepted 5 June 2015
Published online 1 July 2015

Introduction

The multigenic family of UDP-glucuronosyltransferases (UGTs) comprises important drug-metabolizing enzymes for the detoxification of various endogenous compounds (e.g. bile acids, bilirubin, and steroids) and exogenous compounds (e.g. drugs, environmental pollutants, and dietary constituents) (Dutton, 1980; Ritter, 2000). The UGT superfamily has been divided into many subfamilies on the basis of amino acid homology and gene structures. The human UGT superfamily comprises two families (UGT1 and UGT2) and three subfamilies (UGT1A, UGT2A, and UGT2B) (Burchell et al., 1998; Mackenzie et al., 1997, 2005). Each UGT isoform has been shown to exhibit unique substrate and tissue specificities (Kiang et al., 2005; Ritter, 2000; Tukey & Strassburg, 2000).

Human UGT1A6 was previously reported to be mainly expressed in the liver and kidney (Fallon et al., 2013; Harbourt et al., 2012; Ohno & Nakajin, 2009; Tukey & Strassburg, 2000). It has been shown to play important roles in the glucuronidation of planar and small aromatic molecules including acetaminophen and polycyclic aromatic hydrocarbons (Kiang et al., 2005; Radominska-Pandya et al., 1999; Ritter, 2000; Tukey & Strassburg, 2000). In addition, serotonin is regarded as an endogenous substrate for UGT1A6 (Court, 2005). Krishnaswamy et al. (2003) demonstrated that individual variabilities in the expression and function of UGT1A6 in the human liver were marked, with more than 120- and 13-fold variabilities in UGT1A6 protein content and serotonin glucuronidation activities, respectively.

Pigs and minipigs have been used as experimental animals in pharmacological and toxicological studies because many of their physiological characteristics are similar to those of humans (Bode et al., 2010; Khan, 1984). Minipigs (approximately 50 kg body weight for adult animals) are smaller than pigs, and have been developed through selective breeding in order to override the shortcomings associated with large domestic pigs (Khan, 1984). Therefore, minipigs are expected to be becoming a popular alternative to non-rodent experimental species for humans in drug discovery and development.

Many UGT enzymes have been suggested to be expressed in the hepatic and/or extrahepatic tissues of mammals

Address for correspondence: Nobumitsu Hanioka, Department of Biochemical Toxicology, Yokohama University of Pharmacy, 601 Matano-cho, Totsuka-ku, Yokohama 245-0066, Japan. E-mail: nhanioka@hamayaku.ac.jp

including humans, monkeys, and rodents (Mackenzie et al., 1997, 2005; Tukey & Strassburg, 2000). Furthermore, several UGT cDNAs of monkeys, rats, and mice have been cloned (http://www.flinders.edu.au/medicine/sites/clinical-pharmacology/ugt-homepage.cfm), and the functions of each UGT enzyme coded by cDNA have been identified (Kiang et al., 2005; Ritter, 2000). We first reported the cDNA cloning and enzymatic properties of UGT1A1 in minipigs (Miyake et al., 2013); however, minipig UGT cDNAs, except for UGT1A1, have not yet been cloned.

The aim of the present study was to precisely identify similarities and differences in the enzymatic properties of UGT1A6 between humans and minipigs. To achieve this, minipig UGT1A6 (mpUGT1A6) cDNA was cloned by the 3′ and 5′ rapid amplification of cDNA ends (3′-RACE and 5′-RACE, respectively), and the corresponding protein as well as human UGT1A6 (hUGT1A6) enzyme was expressed in insect cells. The enzymatic properties of UGT1A6 were examined by a kinetic analysis for serotonin glucuronidation.

Materials and methods

Materials

Two male minipig livers (14–15 months old, 33–35 kg body weight) were supplied by Kiwa Laboratory Animals (Wakayama, Japan). Pooled minipig liver microsomes (MPLM) from two animals were prepared as described previously (Miyake et al., 2013). Pooled human liver microsomes (HLM, 50 donors) were purchased from XenoTech (Lenexa, KS); the oligo(dT) adaptor primer, 3′-Full Race Core Set, PrimeStar HS DNA Polymerase, Ex Taq HS DNA Polymerase, and *Hin*dIII were from Takara Bio (Otsu, Japan); the pGEM-T vector was from Promega (Madison, WI); the 5′-RACE System, pFastBac1 vector, Bac-to-Bac Baculovirus Expression System, and *Spodoptera frugiperda* (Sf9) cells were from Invitrogen (Carlsbad, CA); serotonin was from Wako Pure Chemical Industries (Osaka, Japan); serotonin glucuronide was from Toronto Research Chemicals (Toronto, Canada); alamethicin was from Sigma-Aldrich (St. Louis, MO); UDP-glucuronic acid was from Nacalai Tesque (Kyoto, Japan); and goat anti-human UGT1A6 antibody was from Santa Cruz Biotechnology (Santa Cruz, CA). Oligonucleotide primers were commercially synthesized at Sigma Genosys (Ishikari, Japan). All other chemicals and reagents used were of the highest quality commercially available.

Sequencing of mpUGT1A6 cDNA

Total RNA of the minipig liver was extracted as described previously (Hanioka et al., 2006). First-strand cDNA was synthesized from total RNA using the oligo(dT) adaptor primer. A partial fragment of mpUGT1A6 cDNA was amplified by a polymerase chain reaction (PCR) from minipig liver first-strand cDNA as a template using forward and reverse primers (Homo-UGT1A6-FP and Homo-UGT1A6-RP, Table 1) that were designed based on two regions in UGT1A6 cDNA, which are highly homologous in different species, such as humans (accession number, NM_001072), monkeys (accession number, AF104337), rats (accession number, NM_057105), and mice (accession number, U16818) in the GenBank database. PCR by PrimeStar HS DNA Polymerase consisted of initial denaturation at 94 °C for 180 s followed by 30 cycles of denaturation at 98 °C for 10 s, annealing at 55 °C for 10 s, and extension at 72 °C for 60 s. The PCR product was introduced into the pGEM-T vector using TA cloning, and sequenced in both the forward and reverse directions.

3′-RACE for mpUGT1A6 cDNA was performed using the 3′-Full Race Core Set according to the protocol of the manufacturer. Gene-specific primers (3′-GSP1 and 3′-GSP2, Table 1) were designed based the nucleotide sequence of a partial fragment of mpUGT1A6 cDNA amplified by PCR using Homo-UGT1A6-FP and Homo-UGT1A6-RP primers. After first-strand cDNA was synthesized from minipig liver total RNA, amplification in the first PCR was primed using first-strand cDNA as a template with 3′-GSP1 and 3′site adaptor primers (3′-SAD, Table 1). PCR by PrimeStar HS DNA Polymerase consisted of initial denaturation at 94 °C for 180 s followed by 30 cycles of denaturation at 98 °C for 10 s, annealing at 56 °C for 5 s, and extension at 72 °C for 240 s. The PCR product was used as a template for nested PCR, and amplification was primed using the primers of 3′-GSP2 and 3′-SAD. PCR by PrimeStar HS DNA Polymerase consisted of initial denaturation at 94 °C for 90 s followed by 30 cycles of denaturation at 98 °C for 10 s, annealing at 56 °C for 5 s, and extension at 72 °C for 240 s. The PCR product was introduced into the pGEM-T vector using TA cloning and sequenced in both the forward and reverse directions.

5′-RACE for mpUGT1A6 cDNA was performed using the 5′-RACE System according to the protocol of the manufacturer. Gene-specific primers (5′-GSP1, 5′-GSP2, and 5′-GSP3,

Table 1. Oligonucleotide primers used for cDNA cloning of mpUGT1A6.

Primer name	Sequence	Target
Homo-UGT1A6-FP	5′-CAACTGCCAGAGCCTCCTG-3′	Partial fragment
Homo-UGT1A6-RP	5′-CACAATTCCATGTTCTCCAGACGCA-3′	
3′-GSP1	5′-GGGAGGCCAAGTTCGATGC-3′	3′-RACE
3′-GSP2	5′-CATTTGGCTGATGAGATACGACTTTGTC-3′	
3′-SAD	5′-CTGATCTAGAGGTACCGGATCC-3′	
5′-GSP1	5′-ATAGGCTTCAAATTC-3′	5′-RACE
5′-GSP2	5′-CAGCCAAATGTCAGCCTTGCGATATAAG-3′	
5′-GSP3	5′-CGGTCGGAGAACGCAGTGTAG-3′	
5′-AAP	5′-GGCCACGCGTCGACTAGTACGGGIIGGGIIGGGIIG-3′	
5′-AUAP	5′-GGCCACGCGTCGACTAGTAC-3′	
mpUGT1A6-FP	5′-AAGCTTAAAATGGCCTGCCTTCTC-3′	Full-length
mpUGT1A6-RP	5′-AAGCTTTCAGTGTGTCTTGGATTTGTG-3′	

Underlined letters are the *Hin*dIII sites.

Table 1) were designed based on the nucleotide sequence of a partial fragment of mpUGT1A6 cDNA amplified by PCR using Homo-UGT1A6-FP and Homo-UGT1A6-RP primers. First-strand cDNA was synthesized from minipig liver total RNA using 5′-GSP1, and the oligo(dC) tail was introduced at the 3′-end. Amplification of the first PCR was primed using oligo(dC) tailed first-strand cDNA with the abridged anchor primer (5′-AAP, Table 1) and 5′-GSP2 primer. PCR by Ex Taq HS DNA Polymerase consisted of initial denaturation at 94 °C for 90 s followed by 30 cycles of denaturation at 94 °C for 35 s, annealing at 55 °C for 60 s and extension at 72 °C for 210 s with a final extension at 72 °C for 360 s. The PCR product was used as a template for nested PCR, and amplification was primed using the abridged universal amplification primer (5′-AUAP, Table 1) and 5′-GSP3 primer. PCR by Ex Taq HS DNA Polymerase consisted of initial denaturation at 94 °C for 90 s followed by 30 cycles of denaturation at 98 °C for 35 s, annealing at 57 °C for 60 s, and extension at 72 °C for 210 s. The PCR product was introduced into the pGEM-T vector using TA cloning and sequenced in both the forward and reverse directions.

Cloning of mpUGT1A6 cDNA

First-strand cDNA was synthesized from total RNA the using oligo(dT) adaptor primer. Full-length mpUGT1A6 cDNA was amplified by PCR using PrimeStar HS DNA Polymerase from minipig liver first-strand cDNA as a template using forward and reverse primers (mpUGT1A6-FP and mpUGT1A6-RP, Table 1). The PCR products of hUGT1A6 and mpUGT1A6 cDNAs were directly introduced into the pGEM-T vector using TA cloning. The cDNA fragments corresponding to hUGT1A6 and mpUGT1A6 were cut from the pGEM-T plasmids with *Hin*dIII and were subsequently subcloned into the pFastBac1 vector digested with *Hin*dIII.

Expression of hUGT1A6 and mpUGT1A6 enzymes

A recombinant baculovirus carrying mpUGT1A6 cDNA as well as hUGT1A6 cDNA (Hanioka et al., 2006) was generated using the Bac-to-Bac Baculovirus Expression System according to the protocol of the manufacturer. Regarding protein expression, Sf9 cells (2.0×10^6 cells/flask) were infected with recombinant baculoviruses at a multiplicity of infection of 1.0. Cells were harvested 72 h post-infection, and the membrane fractions were prepared as described previously (Kokawa et al., 2013).

Assay for serotonin glucuronidation activity

Serotonin glucuronidation activities in the liver microsomes and recombinant UGT1A6 enzymes of humans and minipigs were determined according to a previous study with some modifications (Hanioka et al., 2006). The incubation mixture contained liver microsomes (200 μg protein/mL) or recombinant UGT1A6 enzymes (500 μg protein/mL), serotonin (0.1–20 mM) as a substrate, 10 mM $MgCl_2$, and 20 mM UDP-glucuronic acid in a final volume of 500 μL of 50 mM Tris-HCl buffer (pH 7.4). The substrates were dissolved in 20% methanol. The final concentration of methanol in the incubation mixture was 1% (v/v). Alamethicin (20 μg/mL) was also added to the incubation mixture for liver microsomes.

After preincubation for 2 min at 37 °C, the reaction was initiated by adding UDP-glucuronic acid. Incubation was performed for 20 min at 37 °C and terminated by adding 50 μL of 10% phosphoric acid and vortexing. The samples were centrifuged at 12 000 *g* for 10 min at 4 °C. The supernatant was filtered with a polytetrafluoroethylene membrane filter (0.45 μm), and 20 μL of the filtrate was subjected to high-performance liquid chromatography with an Inertsil ODS-SP column (4.6 mm i.d. × 150 mm; GL Sciences, Tokyo, Japan). The column was maintained at 40 °C. Serotonin glucuronide was isocratically eluted with 20 mM KH_2PO_4 (pH 2.5)/methanol (98:2, v/v) at a flow rate of 1.0 mL/min. Fluorometric detection was performed with an excitation at 225 nm and an emission at 330 nm. Standard curve samples spiked with serotonin glucuronide were prepared in the same manner as incubation samples.

Other methods

The total protein concentrations of recombinant UGT1A6 enzymes were determined with the DC Protein Assay Kit (Bio-Rad Laboratories, Hercules, CA) using bovine serum albumin as a standard. Immunoblotting of recombinant UGT1A6 enzymes (5.0 μg protein/lane for hUGT1A6 and 20 μg protein/lane for mpUGT1A6) as well as liver microsomes (10 μg protein/lane for HLM and 20 μg protein for MPLM) with an anti-human UGT1A6 antibody was performed as described previously (Hanioka et al., 2010).

The glucuronidation activities of recombinant UGT1A6 enzymes toward estradiol at the 3-hydroxy position (3-OH), trifluoperazine, mycophenolic acid, propofol, zidovudine, 7-hydroxy-4-trifluoromethylcoumarin, and 4-methylumbelliferone were determined as described previously (Miyake et al., 2013). Substrate concentrations (estradiol, 20 μM; trifluoperazine, 50 μM; mycophenolic, 200 μM; propofol, 50 μM; zidovudine, 1000 μM; 7-hydroxy-4-trifluoromethylcoumarin, 50 μM; 4-methylumbelliferone, 100 μM) for the determination of glucuronidation activities were set to be similar to the K_m value for each enzyme activity by HLM obtained in a preliminary kinetic analysis. The protein concentrations of recombinant UGT1A6 enzymes for the glucuronidation assay were as follows: 2000 μg protein/mL for estradiol (3-OH), mycophenolic acid, and propofol; 500 μg protein/mL for trifluoperazine; 1000 μg protein/mL for zidovudine; 100 μg protein/mL for 7-hydroxy-4-trifluoromethylcoumarin; and 50 μg protein/mL for 4-methylumbelliferone. The reaction times for the glucuronidation assay were as follows: 60 min for estradiol (3-OH), mycophenolic acid, and zidovudine; 20 min for trifluoperazine; 40 min for propofol; and 10 min for 7-hydroxy-4-trifluoromethylcoumarin and 4-methylumbelliferone.

Data analysis

The kinetic parameters (K_m and V_{max}) for serotonin glucuronidation were calculated by constructing velocity versus substrate concentration (V–$[S]$) plots using SigmaPlot v8.02 software (Systat Software, San Jose, CA). *In vitro* clearance values were CL_{int} (V_{max}/K_m). All values are

expressed as the mean ± S.D. of three separate experiments. Statistical comparisons were made with an unpaired two-tailed Student's *t*-test, and differences were considered significant when $p < 0.05$.

Results

Cloning and sequence analysis of mpUGT1A6 cDNA

Full-length mpUGT1A6 cDNA was obtained by the RACE method. The medium partial cDNA fragment of 535 bp was amplified by PCR from minipig liver first-strand cDNA as a template with primers designed based on the nucleotide sequence homology of UGT1A6 cDNAs in several different species. 3′- and 5′-RACE were then performed, and the nucleotide sequences of 881 and 908 bp were analyzed, respectively. Full-length mpUGT1A6 cDNA contained 1937 bp with an open reading region of 1599 bp encoding the respective protein of 532 amino acids (Figure 1). The cDNA cloned from the minipig liver in this study was named "minipig UGT1A6" by UDP-Glucuronosyltransferase Nomenclature and was registered in GenBank (accession number, LC032361). Amino acid homology between hUGT1A6 and mpUGT1A6 was 79.9% (Figure 2).

Expression of mpUGT1A6 enzyme

The recombinant enzymes of mpUGT1A6 and hUGT1A6 were expressed in insect cells. Figure 3 shows immunoblotting for liver microsomes and the recombinant UGT1A6 enzymes of humans and minipigs using an anti-human UGT1A6 antibody. All enzyme sources, except for the negative control (mock), yielded an immunodetectable UGT1A6 protein. The staining band profile of recombinant hUGT1A6 and mpUGT1A6 enzymes were reproducible in three independent expression experiments.

Enzymatic properties of mpUGT1A6 enzyme

A kinetic analysis of serotonin glucuronidation was performed using recombinant hUGT1A6 and mpUGT1A6 enzymes as well as HLM and MPLM. No activity was detected in the Sf9 cell membranes of the negative control (mock). *V*–[*S*] plots are shown in Figure 4 for liver microsomes and Figure 5 for recombinant UGT1A6 enzymes, respectively. The calculated kinetic parameters are summarized in Table 2. The kinetics of serotonin glucuronidation by the liver microsomes and recombinant UGT1A6 enzymes of humans and minipigs fit the Michaelis–Menten equation. The K_m, V_{max}, and CL_{int} values of human enzymes were 12.9 mM, 30.6 nmol/min/mg protein, and 2.41 μL/min/mg protein for HLM, and 10.5 mM, 4.04 nmol/min/mg protein, and 0.39 μL/min/mg protein for the recombinant hUGT1A6 enzyme, respectively. The K_m and V_{max} values of MPLM were 49% and 75% of HLM, respectively; and the CL_{int} value of MPLM was 1.6-fold that of HLM. In recombinant enzymes, the K_m value of mpUGT1A6 was similar to that of hUGT1A6, whereas the V_{max} and CL_{int} values of mpUGT1A6 were 2.1- and 2.4-folds higher than those of hUGT1A6, respectively.

In order to obtain further information on the enzymatic properties of mpUGT1A6, glucuronidation activities toward typical UGT substrates (estradiol, trifluoperazine, mycophenolic acid, propofol, zidovudine, 7-hydroxy-4-trifluoromethylcoumarin, and 4-methylumbelliferone) in recombinant hUGT1A6 and mpUGT1A6 enzymes were determined (Table 3). Glucuronidation activities toward estradiol (3-OH), mycophenolic acid, 7-hydroxy-4-trifluoromethylcoumarin, and 4-methylumbelliferone in mpUGT1A6 were significantly higher (1.7–5.8-fold) than those of hUGT1A6. Trifluoperazine, propofol, and zidovudine glucuronidation activities were not detected in any recombinant UGT1A6 enzymes of humans and minipigs.

Figure 1. Nucleotide sequence of mpUGT1A6 cDNA. Bold letters are start and stop codons.

```
   1 caagttccagcATGGCCTGCCTTCTCCGGGCGTTTTGGGCAGTTTCTGCAGCGGTTCTCC 60
  61 TCTCAGCACTTTGGGGCACGGTTGCAGGGGACAGGCTGCTGGTGGTCCCTCAGGATGGAA 120
 121 GCCACTGGCTCAGCATGAAGGACATCGTTGTGCGGCTCAGTGAGAAAGGGCACGAGATCG 180
 181 TGGTGGTGGCGCCGGAAATCAACCTGCTTCTCACAGAATCCAAATACTACACCAGGAAGA 240
 241 TCTATCCGGTGCCCTACGACCAGGAGGAGCTGGAGGGCCGTTACCGGTCTTTTGGAAGAA 300
 301 ACCACTTTTCGGAGCGATGGTTGCTGAACGCCGCTCAGGTGGAGTACAGGAATAACATGA 360
 361 TTGTGATCAACATGTACTTCCTCACCTGCCAGAGCCTCCTGAGGGACGCCGCCACCCTGA 420
 421 GCTTCCTCCGGGAGGCCAAGTTCGATGCCCTGTTCACAGACCCGGCCTTACCCTGCGGGG 480
 481 TGATCCTGGCCGAGTACCTGGGCCTGCCGTCCGTGTACCTCTTCAGGGGCTTCCCGTGCT 540
 541 CCCTGGAGAACACGTTCACCAGGACCCCAAGCCCCACGTCCTACGTCCCCAGGTACTACA 600
 601 CTGCGTTCTCCGACCGGATGACTTTCCCCCAACGGGTGGCCAACTTCCTTACTAGGATCT 660
 661 TGGAGAATATCCTCCTTGACCTGCTGTATACTAAGTACGAAGACCTCGCACGTGATATCC 720
 721 TCAAGATAGAGGTGGACCTACCCGCCTTATATCGCAAGGCTGACATTTGGCTGATGAGAT 780
 781 ACGACTTTGTCTTTGAGTTTCCCCGACCTGTCATGCCCAACATGGTCTTCATTGGAGGGA 840
 841 CCAACTGCAAGAAAGTGGGCGTCCTGTCTCAGGAATTTGAAGCCTATGTAAATGCGTCTG 900
 901 GAGAACATGGAATTGTGGTTTTCTCTTTGGGGTCAATGGTCTCAGAGATTCCGGAGCAGA 960
 961 AAGCTATGGAAATTGCTGATGCTTTGGGCAAAATACCTCAGACAGTCCTCTGGCGCTACA 1020
1021 CTGGGCCTGCACCACCGAATCTTGCCAAGAATACAAAACTCGTCAAGTGGCTGCCCCAAA 1080
1081 ATGATCTGCTTGGTCACCCAAAGGCTCGTGCCTTTATCACGCATTCCGGCTCCCATGGTA 1140
1141 TTTATGAAGGAATATGCAATGGTGTTCCCATGGTGATGATGCCCTTGTTTGGGGATCAGA 1200
1201 TGGATAATGCCAAGCGCATGGAGACCCGGGGAGCTGGAGTGACCTTGAACGTCCTGGAGA 1260
1261 TGACTTCTAAAGATTTGGAAAATGCCCTGAATACTGTCATCAAAGACAAAAGCTATAAGG 1320
1321 AAAACATCATGCGCCTCTCCAGCCTTCACAAGGACCGCCCCATTGAGCCTCTAGACCTGG 1380
1381 CTGTCTTCTGGGTGGAGTTCGTGATGAGGCACAAGGGGGCGCCCCATCTTCGCCCTGCGG 1440
1440 CCCACGACCTCACCTGGTACCAGTACCACTCTTTGGATGTGATCGGCTTCCTCCTGGCGG 1500
1501 TTGGACTGACGGTCGTCTTCATCGCCTTTAAGTGTTGTGTCTTCGCGTACCGGAAATGCT 1560
1561 TTGGGAAAAAAGGGCGAGTGAAGAAATCTCACAAATCCAAGACACACTGAgaggttatag 1620
1621 ccatgctaggtttactgaaccttgccataaagtgacacctcagaatgtttttaaaaaatg 1680
1681 aaaatgatctaattgctcgcctatatagaaagagatatttaaatatcttttctgccccct 1740
1741 ccaatatctttaatctggaccacacttgtcatctttcaaatgactccataggagagctgg 1800
1801 ataggaccctctttcaatctgcaatacctttcctacttagaaatgggatccatagctgcc 1860
1861 cccacctaggatggcaactctaacctcaccttctggcatctaaccatgattatgatagat 1920
1921 tccttcaccaacaatgg 1937
```

Figure 2. Deduced amino acid sequence alignment of hUGT1A6 and mpUGT1A6. Asterisks indicate the same amino acid residues between hUGT1A1 and mpUGT1A1.

```
hUGT1A6     1 MACLLRSFQRISAGVFFLALWGMVVGDKLLVVPQDGSHWLSMKDIVEVLSDRGHEIVVVV 60
mpUGT1A6    1 MACLLRAFWAVSAAVLLSALWGTVAGDRLLVVPQDGSHWLGMKDIVVRLSEKGHEIVVVA 60
              ****** *   ** *** **** * ** ************ *****  **  *******

hUGT1A6    61 PEVNLLLKESKYYTRKIYPVPYDQEELKNRYQSFGNNHFAERSFLTAPQTEYRNNMIVIG 120
mpUGT1A6   61-PEINLLLTESKYYTRKIYPVPYDQEELEGRYRSFGRNHFSERWLLNAAQVEYRNNMIVIN 120
              ** **** ********************  ** *** *** **  * * * *********

hUGT1A6   121 LYFINCQSLLQDRDTLNFFKESKFDALFTDPALPCGVILAEYLGLPSVYLFRGFPCSLEH 180
mpUGT1A6  121 MYFLTCQSLLRDAATLSFLREAKFDALFTDPALPCGVILAEYLGLPSVYLFRGFPCSLEN 180
               **  ***** *  ** *  * ************************************

hUGT1A6   181 TFSRSPDPVSYIPRCYTKFSDHMTFSQRVANFLVNLLEPYLFYCLFSKYEELASAVLKRD 240
mpUGT1A6  181 TFTRTPSPTSYVPRYYTAFSDRMTFPQRVANFLTRILENILLDLLYTKYEDLARDILKIE 240
              ** * * * ** ** ** *** *** *******   **  *   *  *** **  **

hUGT1A6   241 VDIITLYQKVSVWLLRYDFVLEYPRPVMPNMVFIGGINCKKRKDLSQEFEAYINASGEHG 300
mpUGT1A6  241 VDLPALYRKADIWLMRYDFVFEFPRPVMPNMVFIGGTNCKKVGVLSQEFEAYVNASGEHG 300
              **   ** *   ** ***** * ************ ****   ******** *******

hUGT1A6   301 IVVFSLGSMVSEIPEKKAMAIADALGKIPQTVLWRYTGTRPSNLANNTILVKWLPQNDLL 360
mpUGT1A6  301 IVVFSLGSMVSEIPEQKAMEIADALGKIPQTVLWRYTGPAPPNLAKNTKLVKWLPQNDLL 360
              ************** ********************  * *** ** ***********

hUGT1A6   361 GHPMTRAFITHAGSHGVYESICNGVPMVMMPLFGDQMDNAKRMETKGAGVTLNVLEMTSE 420
mpUGT1A6  361 GHPKARAFITHSGSHGIYEGICNGVPMVMMPLFGDQMDNAKRMETRGAGVTLNVLEMTSK 420
              ***  ****** **** ** ************************ ************

hUGT1A6   421 DLENALKAVINDKSYKENIMRLSSLHKDRPVEPLDLAVFWVEFVMRHKGAPHLRPAAHDL 480
mpUGT1A6  421 DLENALNTVIKDKSYKENIMRLSSLHKDRPIEPLDLAVFWVEFVMRHKGAPHLRPAAHDL 480
              ******  ** ****************** ****************************

hUGT1A1   481 TWYQYHSLDVIGFLLAVVLTVAFITFKCCAYGYRKCLGKKGRVKKAHKSKTH 532
mpUGT1A1  481 TWYQYHSLDVIGFLLAVGLTVVFIAFKCCVFAYRKCFGKKGRVKKSHKSKTH 532
              ***************** *** ** ****   **** ******** ******
```

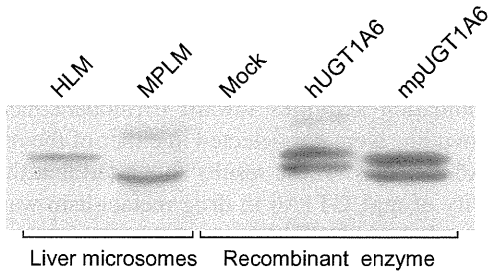

Figure 3. Immunoblotting of liver microsomes and recombinant UGT1A6 enzymes of humans and minipigs. Representative results are shown of pooled samples from three independent preparations. The protein levels applied were 10 μg/lane for HLM, 20 μg/lane for MPLM, 5.0 μg/lane for mock, and recombinant hUGT1A6 enzymes, and 20 μg/lane for the recombinant mpUGT1A6 enzyme.

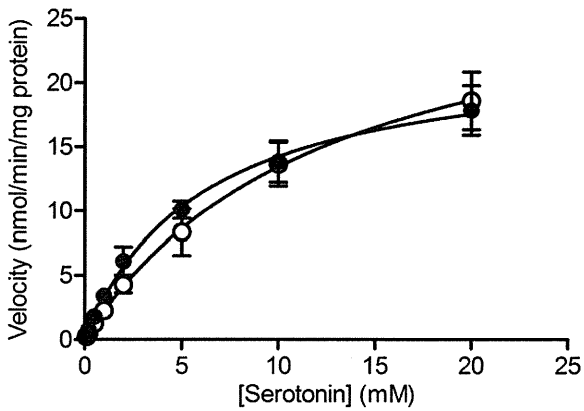

Figure 4. Kinetics of serotonin by HLM and MPLM. Substrate concentrations were 0.1–20 mM. Each point represents the mean ± S.D. of three separate experiments. ○, HLM; ●, MPLM.

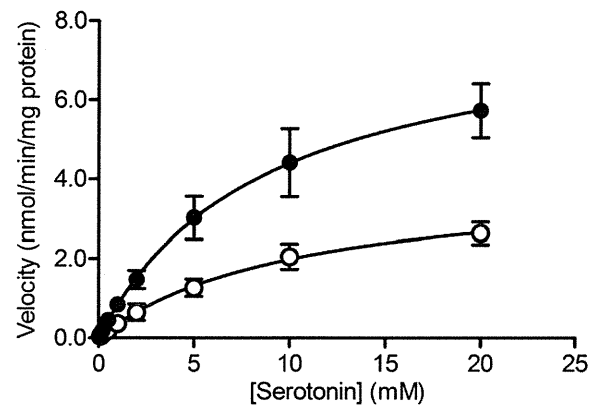

Figure 5. Kinetics of serotonin by recombinant hUGT1A6 and mpUGT1A6 enzymes. Substrate concentrations were 0.1–20 mM. Each point represents mean ± S.D. of three separate experiments. ○, hUGT1A6; ●, mpUGT1A6.

Table 2. Kinetic parameters for serotonin glucuronidation by liver microsomes and recombinant UGT1A6 enzymes of humans and minipigs.

	Liver microsomes		Recombinant enzyme	
	HLM	MPLM	hUGT1A6	mpUGT1A6
K_m (mM)	12.9 ± 2.2	6.26 ± 1.58*	10.5 ± 1.3	8.90 ± 1.09
V_{max} (nmol/min/mg protein)	30.6 ± 69	23.1 ± 2.4*	4.04 ± 0.22	8.29 ± 0.77**
CL_{int} (μL/min/mg protein)	2.41 ± 3.6	3.80 ± 0.62*	0.39 ± 0.06	0.94 ± 0.14**

Each value represents the mean ± S.D. of three separate experiments. Significantly different from HLM or hUGT1A6 (*$p < 0.05$, **$p < 0.01$).

Discussion

UGT1A6 plays a key role in the glucuronidation of drugs, environmental pollutants, and endogenous substances (Kiang et al., 2005; Radominska-Pandya et al., 1999; Ritter, 2000; Tukey & Strassburg, 2000). The regulation of hUGT1A6 function and expression was previously suggested to be influenced by genetic, physiological, and environmental factors (Köhle & Bock, 2009; Mackenzie et al., 2003; Tukey & Strassburg, 2000). Although minipigs are commonly used as an animal model for pharmacological and toxicological studies, little is known about the functions of drug-metabolizing enzymes. In the present study, mpUGT1A6

Table 3. Glucuronidation activities toward various substrates in recombinant UGT1A6 enzymes of humans and minipigs.

	hUGT1A6	mpUGT1A6
Estradiol (3-OH) (20 μM)[b]	0.20 ± 0.06	0.45 ± 0.05**
Trifluoperazine (50 μM)	N.D.	N.D.
Mycophenolic acid (200 μM)[b]	46.9 ± 8.3	80.2 ± 10.0*
Propofol (50 μM)	N.D.	N.D.
Zidovudine (1000 μM)	N.D.	N.D.
7-Hydroxy-4-trifluoromethylcoumarin (50 μM)[a]	2.46 ± 0.27	10.0 ± 0.7**
4-Methylumbelliferone (100 μM)[a]	5.16 ± 0.65	29.7 ± 2.1**

Each value ([a]nmol/min/mg protein; [b]pmol/min/mg protein) represents the mean ± S.D. of three separate experiments. Significantly different from recombinant hUGT1A6 enzymes (*$p < 0.05$, **$p < 0.01$). N.D., not detected.

cDNA was cloned, and the enzymatic properties of mpUGT1A6 expressed in insect cells were examined by a kinetic analysis using serotonin glucuronidation as the probes for the hUGT1A6 enzyme.

We succeeded in cloning full-length mpUGT1A6 cDNA by the RACE method. Previous studies suggested that exon 1 of UGT1As coded the domain for binding of the substrate, while exons 2–5 coded the domain for binding of UDP-glucuronic acid, and that the presence of different possible substrate-binding domains conferred large substrate specificity to UGT1A enzymes (Guillemette et al., 2010; Kiang et al., 2005; Mackenzie et al., 2003; Ritter, 2000; Tukey & Strassburg, 2000). In human UGT1As, the amino acid residues of His38 and Asp150 in exon 1 and His371 and Glu379 in exons 2–5 were found to be conserved among all UGT1A isoforms, and these amino acids were suggested to be key residues for the functional expression of UGT1A enzymes (Court et al., 2003; Li et al., 2007; Patana et al., 2007). The entire coding region of mpUGT1A6 had 80% amino acid sequence identity to that of hUGT1A6, and amino acid residues at the 38, 150, 371, and 379 positions of mpUGT1A6 were the same as the respective positions of human UGT1As.

The expression of UGT1A6 proteins was confirmed by immunoblotting. An anti-human UGT1A6 antibody recognized the corresponding UGT1A6s in liver microsomes and recombinant UGT1A6 enzymes of humans and minipigs. However, the profile and the staining intensity of protein bands were different between liver microsomes and recombinant UGT1A6 enzymes. This phenomenon was attributed to differences in the post-translational modification and/or *N*-glycosylation of UGT1A6 with the endoplasmic reticulum.

The glucuronidation of serotonin is mainly catalyzed by UGT1A6 activity in humans (Court, 2005). The kinetics of serotonin glucuronidation by the liver microsomes and recombinant UGT1A6 enzyme of minipigs as well as humans followed the Michaelis–Menten equation. The K_m value of MPLM was about 50% of that of HLM, and it is considered that the result is due to the difference in the expression ratio of UGT1A6 to total hepatic UGTs between humans and minipigs. The V_{max} and CL_{int} values between HLM and MPLM were ≤ 2-fold, and the significant differences ($p < 0.05$) were detected in a statistical analysis. In recombinant enzymes, the K_m value of mpUGT1A6 was similar to that of hUGT1A6, and the V_{max} and CL_{int} values of mpUGT1A6 were approximately 2-fold those of hUGT1A6. From the kinetic profile and parameter values for the *in vitro* glucuronidation of serotonin, the enzymatic properties of mpUGT1A6 enzyme is suggested to be moderately differed from that of hUGT1A6 enzyme.

We further determined glucuronidation activities toward several UGT substrates each at a single substrate concentration in recombinant hUGT1A6 and mpUGT1A6 enzymes. In humans, the glucuronidation of estradiol (3-OH), trifluoperazine, mycophenolic acid, propofol, and zidovudine has been regarded as mainly being catalyzed by UGT1A1, UGT1A4, UGT1A8, UGT1A9, and UGT2B7, respectively (Bernard & Guillemette, 2004; Court, 2005; Court et al., 2003; Ghosal et al., 2004; Kiang et al., 2005; Ritter 2000; Soars et al., 2003; Zhou et al., 2011). 7-Hydroxy-4-trifluoromethylcoumarin and 4-methylumbelliferone have been reported to be glucuronidated by almost all UGT1A and UGT2B isoforms, except for UGT1A4 (Ghosal et al., 2004; Uchaipichat et al., 2004). Among the UGT substrates examined, mpUGT1A6 and hUGT1A6 were capable of glucuronidating estradiol (3-OH), mycophenolic acid, 7-hydroxy-4-trifluoromethylcoumarin, and 4-methylumbelliferone, and activities were significantly higher in mpUGT1A6 than in hUGT1A6. Glucuronidation activities toward trifluoperazine, propofol, and zidovudine were not detected in either of the recombinant UGT1A6 enzymes. These results suggested that the substrate specificity of mpUGT1A6 in drug metabolism was generally similar to that of hUGT1A6.

We recently cloned full-length minipig UGT1A1 (mpUGT1A1) cDNA, and characterized the function of the mpUGT1A1 enzyme (Miyake et al., 2013). Amino acid homology between hUGT1A1 and mpUGT1A1 was 81%. Estradiol (3-OH) glucuronidation by the recombinant enzymes of mpUGT1A1 and hUGT1A1 showed allosteric sigmoidal kinetics, and no significant differences were observed in S_{50}, V_{max}, Hill coefficient, or *in vitro* clearance (CL_{max}) values between hUGT1A1 and mpUGT1A1. Furthermore, we previously reported that the enzymatic properties of cynomolgus monkey UGT1A6 markedly differed from those of hUGT1A6; however, the amino acid homology of UGT1A6 between humans and cynomolgus monkeys was high (96%) (Hanioka et al., 2006). The results of the present study in combination with our previous findings imply that the enzymatic function of UGT1A6 of minipigs rather than cynomolgus monkeys is similar to that of humans, and also that minipigs are a promising experimental animal for drug metabolism and toxicology research.

Conclusions

Full-length mpUGT1A6 cDNA was cloned by the RACE method for the first time. The recombinant enzymes of mpUGT1A6 and hUGT1A6 expressed in insect cells were prepared, and a kinetic analysis of serotonin glucuronidation by recombinant UGT1A6 enzymes was performed. The kinetics of serotonin glucuronidation by hUGT1A6 and mpUGT1A6 fit the Michaelis–Menten equation. The K_m value of mpUGT1A6 was similar to that of hUGT1A6, whereas the V_{max} and CL_{int} values of mpUGT1A6 were approximately 2-fold higher than those of hUGT1A6.

These results suggest that the enzymatic properties of UGT1A6 enzymes are moderately different between humans and minipigs.

Declaration of interest

The authors report that they have no conflicts of interest. This work was supported in part by a Grant-in-Aid for Scientific Research (26281028) from the Japan Society for the Promotion of Science.

References

Bernard O, Guillemette C. (2004). The main role of UGT1A9 in the hepatic metabolism of mycophenolic acid and the effects of naturally occurring variants. Drug Metab Dispos 32:775–8.

Bode G, Clausing P, Gervais F, et al.; Steering Group of the RETHINK Project. (2010). The utility of the minipig as an animal model in regulatory toxicology. J Pharmacol Toxicol Methods 62:196–220.

Burchell B, Brierley CH, Monaghan G, Clarke DJ. (1998). The structure and function of the UDP-glucuronosyltransferase gene family. Adv Pharmacol 42:335–8.

Court MH. (2005). Isoform-selective probe substrates for *in vitro* studies of human UDP-glucuronosyltransferases. Methods Enzymol 400: 104–16.

Court MH, Krishnaswamy S, Hao Q, et al. (2003). Evaluation of 3′-azido-3′-deoxythymidine, morphine, and codeine as probe substrates for UDP-glucuronosyltransferase 2B7 (UGT2B7) in human liver microsomes: specificity and influence of the UGT2B7*2 polymorphism. Drug Metab Dispos 31:1125–33.

Dutton DJ. (1980). Glucuronidation of drugs and other compounds. Boca Raton (FL): CRC Press.

Fallon JK, Neubert H, Goosen TC, Smith PC. (2013). Targeted precise quantification of 12 human recombinant uridine-diphosphate glucuronosyl transferase 1A and 2B isoforms using nano-ultra-high-performance liquid chromatography/tandem mass spectrometry with selected reaction monitoring. Drug Metab Dispos 41:2076–80.

Ghosal A, Hapangama N, Yuan Y, et al. (2004). Identification of human UDP-glucuronosyltransferase enzyme(s) responsible for the glucuronidation of posaconazole (Noxafil). Drug Metab Dispos 32:267–71.

Guillemette C, Lévesque E, Harvey M, et al. (2010). UGT genomic diversity: beyond gene duplication. Drug Metab Rev 42:24–44.

Hanioka N, Takeda Y, Jinno H, et al. (2006). Functional characterization of human and cynomolgus monkey UDP-glucuronosyltransferase 1A6 enzymes. Chem Biol Interact 164:136–45.

Hanioka N, Tanabe N, Jinno H, et al. (2010). Functional characterization of human and cynomolgus monkey UDP-glucuronosyltransferase 1A1 enzymes. Life Sci 87:261–8.

Harbourt DE, Fallon JK, Ito S, et al. (2012). Quantification of human uridine-diphosphate glucuronosyl transferase 1A isoforms in liver, intestine, and kidney using nanobore liquid chromatography-tandem mass spectrometry. Anal Chem 84:98–105.

Khan MA. (1984). Minipig: advantages and disadvantages as a model in toxicity testing. Int J Toxicol 3:337–42.

Kiang TK, Ensom MH, Chang TK. (2005). UDP-glucuronosyltransferases and clinical drug-drug interactions. Pharmacol Ther 106: 97–132.

Kokawa Y, Kishi N, Jinno H, et al. (2013). Effect of UDP-glucuronosyltransferase 1A8 polymorphism on raloxifene glucuronidation. Eur J Pharm Sci 49:199–205.

Köhle C, Bock KW. (2009). Coordinate regulation of human drug-metabolizing enzymes, and conjugate transporters by the Ah receptor, pregnane X receptor and constitutive androstane receptor. Biochem Pharmacol 77:689–99.

Krishnaswamy S, Duan SX, Von Moltke LL, et al. (2003). Validation of serotonin (5-hydroxtryptamine) as an *in vitro* substrate probe for human UDP-glucuronosyltransferase (UGT) 1A6. Drug Metab Dispos 31:133–9.

Li D, Fournel-Gigleuxs, Barré L, et al. (2007). Identification of aspartic acid and histidine residues mediating the reaction mechanism and the substrate specificity of the human UDP-glucuronosyltransferases 1A. J Biol Chem 282:36514–24.

Mackenzie PI, Bock KW, Burchell B, et al. (2005). Nomenclature update for the mammalian UDP glycosyltransferase (UGT) gene superfamily. Pharmacogenet Genomics 15:677–85.

Mackenzie PI, Gregory PA, Gardner-Stephen DA, et al. (2003). Regulation of UDP glucuronosyltransferase genes. Curr Drug Metab 4:249–57.

Mackenzie PI, Owens IS, Burchell B, et al. (1997). The UDP glycosyltransferase gene superfamily: recommended nomenclature update based on evolutionary divergence. Pharmacogenetics 7: 255–69.

Miyake Y, Mayumi K, Jinno H, et al. (2013). cDNA cloning and functional analysis of minipig uridine diphosphate-glucuronosyltransferase 1A1. Biol Pharm Bull 36:452–61.

Ohno S, Nakajin S. (2009). Determination of mRNA expression of human UDP-glucuronosyltransferases and application for localization in various human tissues by real-time reverse transcriptase-polymerase chain reaction. Drug Metab Dispos 37:32–40.

Patana AS, Kurkela M, Goldman A, Finel M. (2007). The human UDP-glucuronosyltransferase: identification of key residues within the nucleotide-sugar binding site. Mol Pharmacol 72:604–11.

Radominska-Pandya A, Czernik PJ, Little JM, et al. (1999). Structural and functional studies of UDP-glucuronosyltransferases. Drug Metab Rev 31:817–99.

Ritter JK. (2000). Roles of glucuronidation and UDP-glucuronosyltransferases in xenobiotic bioactivation reactions. Chem Biol Interact 129:171–93.

Soars MG, Ring BJ, Wrighton SA. (2003). The effect of incubation conditions on the enzyme kinetics of UDP-glucuronosyltransferases. Drug Metab Dispos 31:762–7.

Tukey RH, Strassburg CP. (2000). Human UDP-glucuronosyltransferases: metabolism, expression, and disease. Annu Rev Pharmacol Toxicol 40:581–616.

Uchaipichat V, Mackenzie PI, Guo XH, et al. (2004). Human UDP-glucuronosyltransferases: isoform selectivity and kinetics of 4-methylumbelliferone and 1-naphthol glucuronidation, effects of organic solvents, and inhibition by diclofenac and probenecid. Drug Metab Dispos 32:413–23.

Zhou J, Tracy TS, Remmel RP. (2011). Correlation between bilirubin glucuronidation and estradiol-3-gluronidation in the presence of model UDP-glucuronosyltransferase 1A1 substrates/inhibitors. Drug Metab Dispos 39:322–9.